Computational Methods For The Black Hole Imaging

Jiahui Tang
Massachusetts Institute of Technology
77 Massachusetts Ave, Cambridge, MA 02139
jiahuita@mit.edu

Abstract

This project aims to study some of the image reconstruction methods developed for the Very Long Baseline Interferometry (VLBI) data. Observation of distant, non-visual cosmic objects is often challenged by the diffraction limit of telescopes. Interferometry essentially overcomes this by observing in the frequency domain, but due to various limits (number of telescope dishes, atmospheric inconsistency, etc.) the data is very sparse and noisy. Different image reconstructions methods are proposed which stand behind different assumptions of the data. We aim to give a comprehensive comparisons of different regularized maximum likelihood (RML) algorithms on synthetic data of the milky way galaxy black hole SgrA from VLBI imaging challenge. After evaluation, we selected the set of best performing parameters, which is BSMEM, applying that to reconstruct image. Besides, we also tried several other image prior assumptions such as ring shape, polarization, rotation, and multi frequency to reconstruct different SgrA* image, and displayed our reconstruction results in this report.*

1. Introduction

1.1. Very Long Baseline Interferometry

Very long baseline interferometry (VLBI) refers to using multiple telescopes to emulate samples from a single large telescope with diameter equal to the maximum distances between telescopes in the array.

Classic optics states that the angular resolution of a telescope is limited by its diameter and the incident wavelength, that is, $\theta \sim \frac{\lambda}{D}$. To achieve higher resolving power at radio frequency, one must employ an extremely large telescope dish, which is nearly impossible in engineering terms. Interferometry, however, gets around this problem since it is the baseline length between 2 telescopes that dictates its resolving power. By forming an array of telescopes globally, we are able to jointly use results from different baselines to acquire images of distant objects. More details about baseline interferometry can be found at [5].

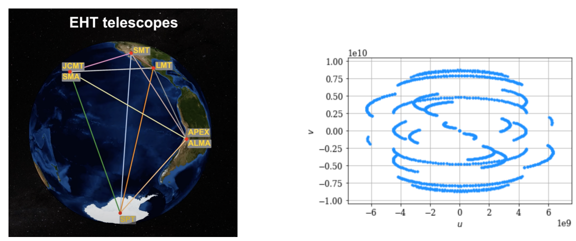

Figure 1. EHT telescopes and Earth Rotation Synthesis
The left image shows EHT telescopes around the world. Images from [12]. Each pair of telescopes form a baseline. As the Earth rotates, each baseline forms a pair of symmetrical elliptical shape, shown on the right.

1.2. Event Horizon Telescope

One domain for the application of VLBI measures is to image the immediate environment around a blackhole's with angular resolution comparable to its event horizon. The Event Horizon Telescope [2] is an international initiative to collaboratively capture images of black holes using a virtual earth-sized telescope, by linking together existing telescopes using novel systems. Its goal is to leverage global collaboration to create new instructions with angular resolving power at short wavelengths that are highest possible from the surface of the earth. The first image of a blackhole is captured using VLBI reconstruction algorithms in the galaxy Messier 87 in the center of the Virgo A galaxy.

In this project, we will evaluate the performance of various reconstruction algorithms on EHT data based on training and testing data from EHT Imaging Challenge [4]. This could better help researchers understand bias of each imaging algorithm, and develop better and robust algorithms to reconstruct an image for SgrA*, our Milky Way Galaxy's blackhole, which is said to be more challenging than M87.

1.3. Earth Rotation Synthesis

Given K telescopes, we could produce $\binom{K}{2}$ baselines, each with a unique spatial frequency components that can be visualized in a 2D plot with x axis representing East-West frequency (**u**), and y axis representing North-South frequency (**v**). Due to Earth's self-rotation, the angle between a baseline and the direction of the source ($\hat{s}$) changes, so a single baseline could produce an elliptical-shaped track of u-v pairs. This is called earth rotation synthesis [9], depicted in Fig.1, and allows us to cover more spatial frequencies in the u-v frequency plane.

1.4. Image Reconstruction

The VLBI operates in the spatial frequency domain, so the actual image needs to be reconstructed from its raw data. The reconstruction algorithm for VLBI measurements is an on-going research field. An ideal algorithm could find an explanation that respects prior assumptions while still satisfying the observed data, among an infinite number of possible image assumptions that explain the data.

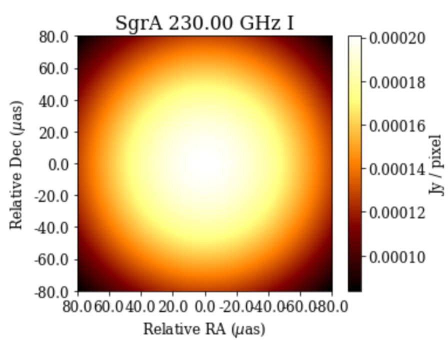

Figure 2. An example empty disk shape prior for Sgr A* with flat background and Gaussian core

Besides, the algorithm should also be able to reconstruct images in fine angular resolution at the mm/sub-mm wavelengths, while at the same time be robust to the additional measurement errors due to rapidly changing inhomogeneities in various telescopes' atmosphere environments. The section 2 of this report contains an overview of these algorithms.

2. Related Work

The challenge of image reconstruction is that reconstructed images are not unique. Reconstructions require prior assumptions, information and constraints. Some strong constraints are image positivity, restricted field of view (FOV). While prior assumptions could favor some physically motivated properties such as image smoothness, entropy, sparsity, or maximum resolution of reconstruction features [8].

Such algorithms could be broadly classified into two methodologies, which are inverse modeling and forward modeling. The former approach includes deconvolution methods such as CLEAN; the latter includes regularized maximum likelihood (RML) algorithms such as maximum entropy method (MEM) [8].

2.1. Inverse Modeling

Inverse modeling begins with an inverse Fourier transform of sampled image, after which the algorithm deconvolves the effects with the limited baseline coverage.

CLEAN: The CLEAN algorithm dates back to 1974 [5]. The essence of it revolves around an iterative procedure that locates the point with highest reconstructed intensity and removes the point-source response at that location. This is due to the fact that the "dirty beam" (i.e. the inverse Fourier Transform of sampling function in the spatial frequency domain) contains sidelobes caused by sparse sampling. Several improvements have been proposed based on CLEAN [6].

2.2. Forward Modeling

Forward modeling represents an image as an array of pixels, and apply Fourier transform of this array to evaluate consistency between data and image. Forward modeling approaches have been intensively developed for EHT.

MEM: The Maximum Entropy Method defines a target entropy function that is determined solely by the image intensity [5]. In reconstructing the image, it also aims to maximize the entropy with the restraint that the Fourier Transform of the reconstructed image must fit the observed visibility values. The selection of entropy function largely dictates the outcome of the algorithm and is intended to introduce as little details in the unmeasured area as possible.

BSMEM: The BiSpectrum Maximum Entropy Method uses a fully Bayesian approach to find the best possible image by using the entropy as a prior [7]. In searching for the image, gradient descent method is used to iteratively optimize the image and narrow down the search range.

SQUEEZE: This algorithm takes a Markov chain Monte Carlo method to sample images from posterior distribution. It is not limited in its choice of regularizers or constraints, but comes with a large number of parameters to finetune [10].

CHIRP: The Continuous High-resolution Image Reconstruction using Patch Priors (CHIRP) algorithm takes a Bayesian approach with improved forward model approximation to better model spatial frequency measurement. Meanwhile, it could model atmospheric noise with simpler problem formulation and optimization strategy [10].

2.3. Open Source Software Packages

Three open source software packages are used with scripted imaging pipelines in the second stage creation of the first M87 EHT result. Each pipeline has some fixed choices (e.g., the convergence criterion, the pixel size, etc.) but takes additional parameters (e.g., the regularizer weights, the total compact flux density) as arguments. [10]

DIFMAP: a scripted version of the CLEAN algorithm to carry out the parameter search. [11]

EHT-imaging: a RML method that uses a template imaging script that use MEM, L1 norm, total variation (TV) and total squared variation (TSV) as regularizers. [1]

SMILI: a RML method that reconstruct image using low-band EHT data that use L1, TV, TSV regularizers. [3]

In this research, we leveraged on *EHT-imaging* package to experiment different algorithms, as it is built in Python and easily accessible, which also supports multiple algorithms and regularizers for fine tuning.

3. Approach

To evaluate different algorithms, we tested image reconstruction algorithms on a suite of synthetic dataset, so that we could optimize the algorithm with objective performance assessment and compare it against groundtruth data.

The objective function for RML algorithm is

$$J(I) = \sum \alpha_D \chi^2_D(I, d) - \sum \beta_R S_R(I)$$

where the $\chi^2_D(I, d)$ is the data term, and $S_R(I)$ is the regularizer, which are two primary hyper-parameters to tune.

To be specific, using the EHT challenge dataset, we reconstruct synthetic data from a large survey of imaging parameters supported by *eht-imaging*, and use grid search to tune different combinations of hyper-parameters of data term and regularizers.

Below is a list of possible data terms and regularizers we experimented with.

Data term	vis, bs, amp, cphase, cphase_diag, camp, logcamp, logcamp_diag
Regularizer	simple, gs, tv, tv2, l1w, lA, patch, compact, compact2, rgauss

It could be uninformative in highly degraded VLBI reconstruction to use traditional pixel-wise error metrics such as MSE and PSNR. Thus, after experiments, we conducted a fair quantitative comparison of the results with the corresponding ground truth images by comparing there metrics, which are normalized cross correlation (*nxcorr*), normalized root mean squared error (*nrmse*) and square root of the sum of squared differences (*rssd*). This allows us to select and evaluate parameters to use in EHT tasks.

Below Fig 3 is a plot of ground truth synthetic data of Sgr A* blackhole image and its dirty beam.

Another popular alternative metrics is the perceptually motivated structural similarity (SSIM) index measure proposed by Katherine et al. [10], which is not yet supported in *eht-imaging*, so it is not used for evaluation here.

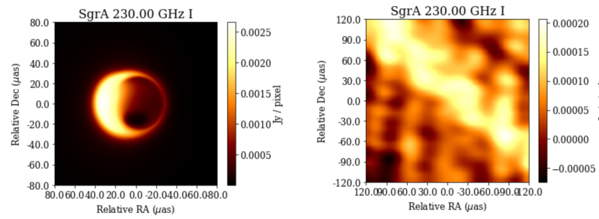

Figure 3. Left: Groundtruth Synthetic Image of Sgr A*; Right: Dirty Beam

4. Experimental Results

For evaluation, three metrics are used to evaluate different algorithms by comparing ground truth synthetic data with the reconstructed images. By ranking *nxcorr* in ascending, or *nrmse* and *rssd* in descending order, it produces the same set of best performing hyper-parameters in our experiment. Below is a snippet of top 10 best performing algorithms.

	nxcorr	nrmse	rssd
(bs, simple)	0.897626	0.466008	1.277258e-13
(bs, lA)	0.895150	0.469276	1.286215e-13
(bs, gs)	0.894336	0.470849	1.290527e-13
(bs, tv2)	0.892311	0.472694	1.295582e-13
(bs, patch)	0.892311	0.472695	1.295585e-13
(bs, rgauss)	0.892301	0.472718	1.295650e-13
(bs, compact2)	0.892301	0.472718	1.295650e-13
(bs, compact)	0.892301	0.472718	1.295650e-13
(amp, l1w)	0.815637	0.569099	1.559816e-13
(amp, patch)	0.803764	0.590276	1.617859e-13

Figure 4. Top 10 Best Performing Hyperparameters and Metrics

We could see that data term Bispectrum (bs) and regularizer Maximum Entropy ($simple$) displays superior result in our experiment.

With this set of best performing hyperparameters, we reconstructed our Sgr A* blackhole image using The BiSpectrum Maximum Entropy Method (BSMEM) as below in Fig 5.

Some other sets of prior assumptions are also explored for reconstruction, including ring shape, polarization, rotation and multi-frequency, results shown below.

5. Conclusion

To conclude, this research shows reconstructing VBLI image still remains a challenging task, as no previous comparable VLBI image of blackhole are seen. From the experiment, we showed that different prior assumptions leads

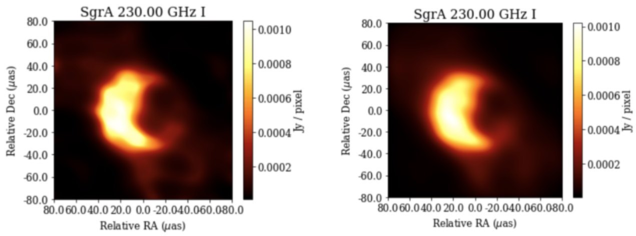

Figure 5. Reconstructed Image of Sgr A* using BSMEM (left) and BSMEM + blurring with fitted beam (right)

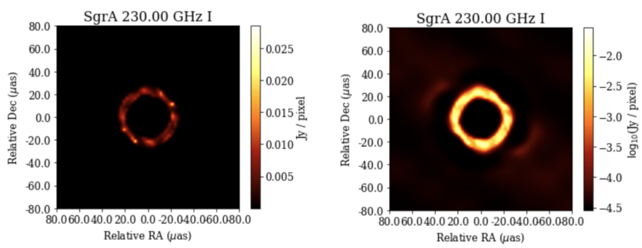

Figure 6. Reconstructed Sgr A* with ring structure (left) and ring in log scale (right)

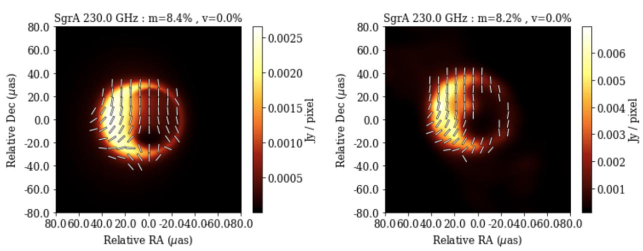

Figure 7. Reconstructed Sgr A* with polarization

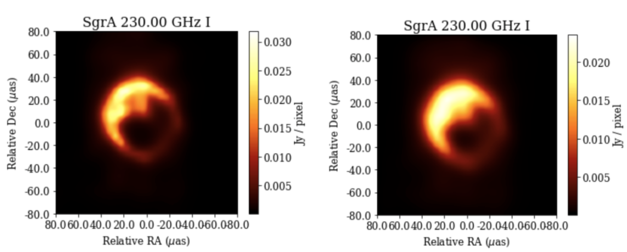

Figure 8. Reconstructed Sgr A* with rotation of u,v coordinates

to different reconstructed photos. By tuning parameters of regularizers and data term, we observe that BSMEM algorithm displaying superior performance among all.

With synthetic data of Sgr A*, we need carefully designed metrics for evaluating reconstruction results to avoid bias. Some other possible metrics is Structural Similarity Index Measure (SSIM), which is not yet supported in *eht-*

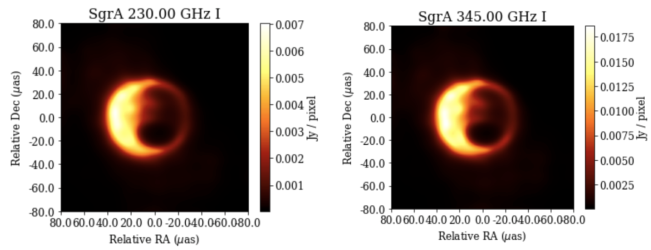

Figure 9. Reconstructed Sgr A* using multi-frequency. 230 GHz (left) and 345 GHz (right)

imaging package's image comparison method, and could be a future direction. For future researcg work with Sgr A* real data, as Sgr A* is a galaxy that is much smaller than M87 but with faster dynamics, it poses further challenges for researchers. Research group shall still blindly work in separate groups to access human bias.

References

[1] Eht-imaging open source package. https://github.com/achael/eht-imaging. 3

[2] Event horizon telescope (eht) group. https://eventhorizontelescope.org/. 1

[3] Smili open source package. https://github.com/astrosmili/smili. 3

[4] Vlbi reconstruction dataset. http://vlbiimaging.csail.mit.edu/. 1

[5] A. R. Thompson, J. M. Morgan, and G. W. Swenson Jr. *Interferometry and Synthesis in Radio Astronomy*. Springer Open, 2017. 1, 2

[6] Alan Bridle. The 'clean' algorithm. https://www.cv.nrao.edu/~abridle/deconvol/node7.html, 1996. 2

[7] David B. Buscher. Direct maximum-entropy image reconstruction from the bispectrum. *Proceedings of the International Astronomical Union*, page 158:91, January 1994. 2

[8] The Event Horizon Telescope Collaboration et al. First m87 event horizon telescope results. iv. imaging the central supermassive black hole. *The American Astronomical Society.*, 2019. 2

[9] Dale E. Gary. Fourier synthesis imaging, radio astronomy, March 2019. 2

[10] Daniel Zoran Vincent L. Fish Sheperd S. Doeleman Katherine L. Bouman, Michael D. Johnson and William T. Freeman. Computational imaging for vlbi image reconstruction. *The IEEE Conference on Com- puter Vision and Pattern Recognition (CVPR)*, 2016. 2, 3

[11] T. J. Person M. C. Shepherd and G. B. Taylor. Difmap: An interactive program for synthesis imaging. *Bulletin of the Astronomical Society*, 26:987–989, 1994. 3

[12] Frankfurt Relastro @ ITP Goethe University. Using vlbi to create an image of the black hole in the center of our galaxy. https://www.youtube.com/watch?v=VnsZj9RvhFU. 1